CellPress

Structure
Article

Structural and Mechanistic Paradigm of Leptin Receptor Activation Revealed by Complexes with Wild-Type and Antagonist Leptins

Kedar Moharana,[1] Lennart Zabeau,[2] Frank Peelman,[2] Philippe Ringler,[3] Henning Stahlberg,[3] Jan Tavernier,[2,*] and Savvas N. Savvides[1,*]

[1]Unit for Structural Biology, Laboratory for Protein Biochemistry and Biomolecular Engineering (L-ProBE), Ghent University, 9000 Ghent, Belgium

[2]Flanders Institute for Biotechnology (VIB) and Department of Medical Protein Research, Ghent University, 9000 Ghent, Belgium

[3]Center for Cellular Imaging and NanoAnalytics (C-CINA), Biozentrum, University of Basel, 4003 Basel, Switzerland

*Correspondence: jan.tavernier@vib-ugent.be (J.T.), savvas.savvides@ugent.be (S.N.S.)

http://dx.doi.org/10.1016/j.str.2014.04.012

SUMMARY

Leptin activates its cognate receptor (LR) to regulate body weight and metabolically costly processes, such as reproduction and immune responses. Despite such benevolent pleiotropy, leptin-mediated signaling has been implicated in autoimmune diseases and breast cancer, thereby rejuvenating interest in leptin antagonism. We present comparative biochemical and structural studies of the LR ectodomain (LR_{ecto}) in complex with wild-type and antagonist leptin variants. We show that high-affinity binding of leptin to the cytokine receptor homology 2 domain of LR_{ecto} primes interactions with the Ig-domain (LR_{Ig}) of another leptin-bound LR_{ecto} to establish a quaternary assembly. In contrast, antagonist leptin variants carrying mutations at the LR_{Ig} binding site only enable binary complexes with LR_{ecto}. Acetylation of free cysteines in LR_{ecto} also abrogates quaternary complexes, suggesting a functional role for intrareceptor disulfides. We propose a revised conceptual framework for LR activation whereby leptin activates predimerized LR at the cell surface to seed higher order complexes with 4:4 stoichiometry.

INTRODUCTION

Leptin receptor (LR), a type I cytokine receptor, is activated by its cognate ligand leptin secreted by the adipose tissue to regulate a host of essential body functions, such as the homeostasis of body weight and energy (Friedman and Halaas, 1998; Halaas et al., 1995; Varela and Horvath, 2012), the immune system and hematopoiesis (Carbone et al., 2012; Procaccini et al., 2012), reproduction and fetal development (Hausman et al., 2012), angiogenesis (Cao et al., 2001; Park et al., 2001), and bone formation (Motyl and Rosen, 2012). Leptin-mediated activation of LR signals through the Janus kinase (JAK)/signal transducer and activator of transcription (STAT) pathways and also modulates the activity of phosphoinositide 3-kinase, mitogen-activated protein kinase, extracellular signal-related kinase, and AMP-activated protein kinase (Wauman et al., 2008). The pleiotropic signaling via the leptin-LR axis and its potential in treating a number of pathologies have been a cynosure for more than a decade. Although leptin monotherapy has been ineffective to curb obesity, it has found applications in type 1 and type 2 diabetes (Cummings et al., 2011; Wang et al., 2010), in rare cases of congenital leptin deficiency (Ramachandrappa and Farooqi, 2011), as a potential antidepressant (Lu et al., 2006), and as a biomarker in breast cancer progression (Artac and Altundag, 2012). The possible involvement of leptin in autoimmune diseases such as multiple sclerosis (De Rosa et al., 2007), rheumatoid arthritis (Otvos et al., 2011), and autoimmune hepatitis (Sennello et al., 2005), and in cancer (Otvos et al., 2011), has raised therapeutic interest in leptin and LR antagonists.

The LR ectodomain (LR_{ecto}) comprises two cytokine receptor homology domains (CRH1 and CRH2) flanking an immunoglobulin (Ig)-like motif, followed by two membrane-proximal fibronectin type III (FNIII) domains (Figure 1A). A single-helix transmembrane domain connects LR_{ecto} to the intracellular segments, which carry the conserved juxtamembrane motifs box1 and box2 for binding of JAKs (Ghilardi and Skoda, 1997). The CRH2 domain is responsible for leptin binding (Fong et al., 1998; Iserentant et al., 2005; Peelman et al., 2004), while the Ig-like domain is required for receptor activation (Zabeau et al., 2004). Whereas LR has been classified as a type 1 cytokine receptor because of the presence of conserved WSXWS sequence motifs in such receptors, it exhibits a number of distinct organizational features suggesting that it may employ unique assembly and mechanistic principles. For instance, LR does not recruit a coreceptor in the signaling complex, it can undergo ligand-independent oligomerization at the cell surface, it has multiple isoforms that may assemble as hetero-oligomers (Bacart et al., 2010), the N-terminal CRH1 segment has a hitherto unidentified role in receptor activation, and LR_{ecto} harbors an unprecedented combination of CRH, Ig-like, and FNIII domains. These architectural eccentricities are manifested at the mechanistic level as well, which is not well understood but was shown to involve preoligomeric receptors at the cell surface (Biener et al., 2005; Couturier and Jockers, 2003) that upon leptin

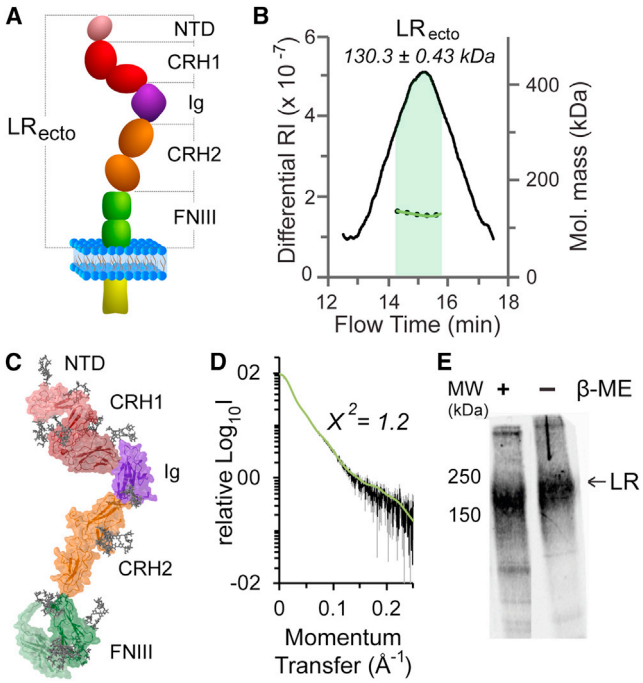

Figure 1. Biochemical and Structural Characterization of LR_{ecto}

(A) Schematic representation of LR. LR_{ecto} has five functional domains: distal NTD (sepia), CRH1 (red), Ig-like domain (violet), and CRH2 (orange), followed by two membrane-proximal FNIII domains (green).

(B) FFF-MALS analysis of LR_{ecto}.

(C) Model for LR_{ecto} based on restrained rigid-body refinement based on SAXS data.

(D) Comparison of calculated X-ray scattering (green) from the rigid-body model of LR_{ecto} against the experimental scattering data (black).

(E) Western blot analysis of full-length LR showing the absence of covalent dimers at the cell surface.

See also Figures S1 and S5.

binding may oligomerize further to form a signaling-competent complex of higher order (Zabeau et al., 2004).

Homology-based structural analysis of leptin, a monomeric cytokine that adopts a four-helix bundle fold (Zhang et al., 1997), complemented by mutagenesis studies led to proposals for three distinct binding sites on leptin (Iserentant et al., 2005; Niv-Spector et al., 2005; Peelman et al., 2004, 2006). The canonical site II interacts with the CRH2 domain on LR and is essential for high-affinity binding, while site III interacts with the Ig-like domain on LR and likely invokes conformational changes necessary for signal transduction. On the other hand, the role of putative binding site I has been rather controversial because of the lack of robust mutagenesis and functional data to fully substantiate its importance. The relevance of site III of leptin has inspired the design of leptin variants with potent antagonistic properties (Gertler, 2006; Peelman et al., 2004), whereby the leptin variants retain their ability to interact with LR but are unable to support signaling. Besides their therapeutic potential, such leptin variants could serve as excellent tools to probe structural and mechanistic aspects of leptin-LR signaling.

Despite great progress in our understanding of the structural basis of several extracellular signaling assemblies mediated by type I cytokine receptors such as the interleukin-6 receptor (IL-6R) (Boulanger et al., 2003; Skiniotis et al., 2005), the interleukin-2 receptor and interleukin-15 receptor (Ring et al., 2012; Wang et al., 2005), and the granulocyte macrophage colony-stimulating factor receptor (Hansen et al., 2008), our view of leptin-LR complexes and the mechanism of LR activation has not yet come to full circle despite recent developments (Carpenter et al., 2012; Mancour et al., 2012). We here employ structural, biophysical, biochemical, and cellular studies to study the assembly and mechanistic principles of mouse LR in complex with wild-type leptin (wt-leptin) and leptin variants with antagonistic properties. In light of a wealth of prior studies, we have arrived at a mechanistic proposal for the assembly of leptin-LR signaling complexes, which can now serve as a working paradigm for future mechanistic interrogation of leptin-mediated signaling.

RESULTS

LR_{ecto} Adopts a Monomeric Extended Structure

To enable structural and biophysical studies of the LR_{ecto} and its complexes with leptin and leptin antagonists, we expressed LR_{ecto} (N-terminal domain [NTD], CRH1 domain, Ig-like domain, CRH2 domain, and tandem FNIII domain) (Figure 1A) in transiently transfected human embryonic kidney 293T (HEK293T) cells in the presence of the mannosidase inhibitor kifunensine (Chang et al., 2007) as a recombinant protein construct carrying a C-terminal hexahistidine tag. LR_{ecto} purified via immobilized metal-ion affinity chromatography and size-exclusion chromatography (SEC) could be characterized as a monodisperse species using multiangle laser light scattering (MALS) after sample resolution via field-flow fractionation (FFF) consistent with monomeric glycosylated LR_{ecto} (Figure 1B). In addition, we investigated the possible role of glycosylation in the oligomerization propensity of LR_{ecto} by expressing LR_{ecto} in stably transfected human embryonic kidney 293S (HEK293S) $GnTI^{-/-}$ cells producing LR_{ecto} with homogeneous N-linked $GlcNAc_2Man_5$ glycans and found that it retains its monomeric character.

We subsequently undertook structural studies of LR_{ecto} in solution by small-angle X-ray scattering (SAXS). In the first instance, this allowed us to probe the oligomerization tendency of LR_{ecto} within a broad range of concentrations up to 17 μM (3.1 mg/ml) (Table 1; Figure S1A available online). To facilitate structural modeling of the SAXS data, we first constructed models of LR_{ecto} on the basis of structure-based sequence alignments, homology modeling, and structure-prediction approaches. Our initial strategy was based on ab initio modeling approaches (Franke and Svergun, 2009) and restrained rigid-body refinement protocols (Petoukhov and Svergun, 2005) but failed to lead to models showing good agreement with the experimental data. Given that LR_{ecto} was shown to have 16 N-linked glycosylation sites (Haniu et al., 1998), we expanded our approach to include modeling of oligomannose glycan trees (Bohne-Lang and von der Lieth, 2005) and treated them as individual rigid-body entities with appropriate restraints to LR_{ecto}. We had previously applied a similar approach to structurally characterize large and flexible glycosylated cytokine receptor complexes (Elegheert et al., 2012; Felix et al., 2013). Our structural analysis of LR_{ecto} showed that LR_{ecto} adopts a monomeric

Table 1. SAXS Analysis of LR_{ecto} and wt-Leptin/LR_{ecto} Quaternary and Binary Complexes

Parameter	LR_{ecto}	wt-Leptin/LR_{ecto} Quaternary Complex	wt-Leptin/LR_{ecto} Binary Complex
Data Collection Parameters			
Beamline	ID 14-3, ESRF	SWING, SOLEIL	SWING, SOLEIL
Detector	PILATUS 1M	AVIEX PCCD	AVIEX PCCD
Beam geometry (mm^2)	0.7 × 0.7	0.45 × 0.04	0.45 × 0.04
Wavelength (Å)	0.931	1.54	1.54
q range ($Å^{-1}$)	0.15–6.11	0.06–6.12	0.06–6.12
Exposure time (s)	100 (10 × 10)	1	1
Concentration range (mg/ml)	0.9–3	10 (injected)	10 (injected)
Temperature (K)	293	293	293
Structural Parameters			
I_0 ($Å^{-1}$) (from P[r])	151.6 ± 4.3	0.137	0.067
R_g (Å) (from P[r])	65.4 ± 0.3	87.0	63.9
I_0 ($Å^{-1}$) (from Guinier)	151.3 ± 1.4	0.137	0.067 ± 0.0
R_g (Å) (from Guinier)	63.8 ± 1.6	84.9	61.9 ± 0.2
D_{max} (Å)	219.2 ± 0.7	297.1	216.7
Porod volume estimate, V_p ($Å^3$)	244,025	1,225,451	463,936
Excluded volume, V_{ex} ($Å^3$)	346,000	1,450,000	608,000
Molecular Mass (kDa)			
From I_0	146.4 ± 4.2	305	149.1
From SAXSMoW	138.5	—	—
Protein sequence (Protparam)	93	218	109
Protein sequence + N-glycans	124	280	140
Modeling Parameters			
Symmetry	P1	P2	P1
χ^2 of reference model	1.1	1.2–1.3	1.3
Number of models averaged	20	20	28
DAMAVER NSD (var)	0.808 ± 0.025	—	—
Rigid body modeling	SASREF	SASREF	SASREF
Initial χ^2	1.2	17.4	4.6
Final χ^2	1.2	2.2	3.5
Software/Server			
Data reduction	BSX-CUBE	FOXTROT	FOXTROT
Data processing	PRIMUS	PRIMUS-QT	PRIMUS-QT
Data evaluation	PRIMUS/GNOM	PRIMUS-QT/GNOM	PRIMUS-QT/GNOM
Structure modeling (ab initio)	DAMMIF	DAMMIF	DAMMIF
Structure modeling (rigid body)	SASREF/EOM	SASREF	SASREF

and extended structure measuring ~80 × 80 × 225 Å that is hallmarked by an elbow bend centered at the Ig domain (Figures 1C and 1D; Figure S1B). The N-terminal CRH1 segment can be described by three structural domains, followed by the Ig segment, a CRH2 segment with two domains, and ending with two FNIII domains. A parallel structural study of LR_{ecto} via negative-stain electron microscopy (EM), albeit at inherently much lower sample concentrations, led to class averages bearing features closely resembling the structural models obtained via SAXS (Figure S1C).

Our finding that LR_{ecto} lacks inherent dimerization propensity even at such high concentrations came as a surprise because of previous reports that LR exists in a dimeric form at the cell surface (Biener et al., 2005; Devos et al., 1997; White and Tartaglia, 1999) and that such predimerized assemblies might be mediated by disulfide bridges between LR molecules (Zabeau et al., 2005). In addition, we had also observed that shorter constructs of the extracellular segment of LR ($LR_{CRH1\text{-}Ig\text{-}CRH2}$ or $LR_{Ig\text{-}CRH2}$) showed the tendency to form covalent oligomers. To cross-validate the possible role of covalent receptor-receptor interactions, we selectively captured LR at the cell surface labeled with sulfo-NHS-SS-biotin in the presence of iodoacetamide, followed by detection via western blotting. Our analysis showed LR as a single band corresponding to the monomeric molecular weight (Figure 1E), thereby establishing the noncovalent character of LR at the cell surface. Thus, in the absence of any inherent oligomerization propensity in LR_{ecto}, dimerization of LR at the cell surface is likely driven by the transmembrane

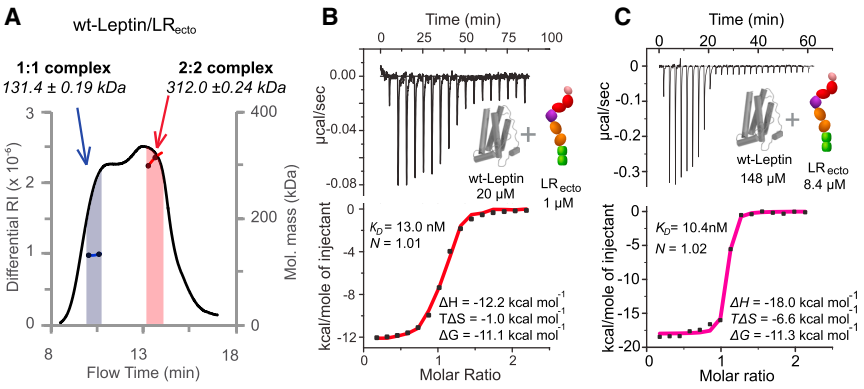

Figure 2. Biochemical and Biophysical Characterization of wt-Leptin/LR$_{ecto}$ Complexes

(A) FFF-MALS analysis of wt-leptin/LR$_{ecto}$ complexes consistent with 1:1 (blue) and 2:2 (red) stoichiometries.

(B) ITC thermograms of wt-leptin binding to LR$_{ecto}$ at concentrations that sustain a 1:1 stoichiometric complex.

(C) ITC thermograms of wt-leptin binding to LR$_{ecto}$ at concentrations that sustain formation of a 2:2 stoichiometric complex.

See also Figure S2.

and intracellular segments of the receptor and may be enhanced by the dimensionality of the membrane (Wu et al., 2011). In this regard, earlier studies investigating constitutive LR dimers at the cell surface demonstrated that the short form of LR lacking the intracellular segment was still able to form constitutive dimers (Biener et al., 2005) and that constitutive dimers consisting of full-length LR are far more stable than LR lacking the intracellular segment (Couturier and Jockers, 2003).

Leptin and LR$_{ecto}$ Engage in a Noncovalent Quaternary Complex with 2:2 Stoichiometry

We used several lines of experimentation to characterize binding of leptin to LR$_{ecto}$ and to obtain structural insights into the assembly of extracellular leptin:LR$_{ecto}$ complexes. Incubation of purified recombinant LR$_{ecto}$ with a molar excess of leptin, followed by chromatographic analysis by SEC, typically resulted in two incompletely resolved peaks: a minor high molecular weight peak and a major low molecular weight peak. This suggested that the leptin-LR$_{ecto}$ complex might be a dynamic equilibrium of high and low molecular weight complexes, with dilution favoring the low molecular weight species. To better characterize these two possible states, we subjected assembled leptin-LR$_{ecto}$ complexes to MALS-FFF analyses and found that the two assemblies are consistent with a binary 1:1 stoichiometry and a quaternary 2:2 complex, respectively (Figure 2A). Subjecting complexes with 2:2 stoichiometry to a new round of SEC resulted in partial dissociation of the 2:2 species to the 1:1 stoichiometric assembly, indicating the concentration dependence of the assemblies in vitro. Both types of stoichiometric complexes could be further stabilized by crosslinking with formaldehyde (Leitner et al., 2010) and isolated by SEC, resulting in better preparative resolution of the two candidate molecular assemblies.

In light of these findings, we sought to characterize the thermodynamic and stoichiometric profile of the leptin-LR interaction by isothermal titration calorimetry (ITC). Our approach centered on carrying out measurements at concentrations that would be representative of those required to maintain the two apparent types of complexes we could identify chromatographically (Figures 2B and 2C). To confirm this, we fractionated the post-ITC protein solutions by SEC and obtained elution profiles that cross-validated the exclusive presence of binary 1:1 complex in the ITC titration at low concentration (Figure S2A). On the other hand, the post-ITC solution at high concentration resolved as a mixture of complexes with 2:2 and 1:1 stoichiometries (Figure S2B), confirming that a 2:2 stoichiometry is the maximum attainable for the leptin-LR$_{ecto}$ complex. Our ITC measurements show that the 1:1 leptin-LR$_{ecto}$ interaction is enthalpically driven and has an equilibrium dissociation constant (K_D) of 13 nM (Figure 2B). Surprisingly, the leptin-LR$_{ecto}$ quaternary complex with 2:2 stoichiometry appears to assemble according to a similar thermodynamic profile (Figure 2C), which in the first instance would discount the notion of a positively cooperative quaternary assembly.

Structural Studies of Leptin in Complex with LR$_{ecto}$

To obtain structural insights into the assembly principles of the leptin-LR$_{ecto}$ complex, we used structural studies by SAXS, which in the first instance served as an orthogonal method for corroborating the molecular sizes of the two apparent stoichiometric complexes of leptin-LR$_{ecto}$ with 1:1 and 2:2 stoichiometries (Table 1). Initial ab initio modeling of SAXS data measured from crosslinked leptin-LR$_{ecto}$ complex with 2:2 stoichiometry (Figure 2A) revealed pronounced features consistent with a particle obeying two-fold symmetry. Indeed, application of P2 symmetry in rigid-body refinement protocols produced the best agreement with the experimental data and revealed a frontally Y-shaped assembly measuring ~225 × 300 × 160 Å composed of two 1:1 leptin-LR$_{ecto}$ subcomplexes (Figure 3A, curve (i), and Figure 3B; Figure S3). In a given 1:1 subcomplex, a leptin molecule binds to the CRH2 domain of LR$_{ecto}$, consistent with what has been termed a site II binding epitope (Peelman et al., 2004), invoking a drastically different conformational state of LR$_{ecto}$ compared with its unbound state. The apparent consequence of such restructuring in LR$_{ecto}$ is that the Ig domain becomes primed to associate with a leptin molecule in the second 1:1 subcomplex to establish a site III binding epitope on leptin (Peelman et al., 2006). Furthermore, the two N-terminal CRH1 segments and the two membrane-proximal FNIII domains extend away from the core of the complex without engaging in homotypic receptor interactions. We note that accounting for 16 N-linked $GlcNAc_2Man_9$ glycans greatly improved model agreement with the scattering data, as recently shown for other receptors (Felix et al., 2013; Guttman et al., 2013). Because attempts to probe structural flexibility in the glycosylated leptin-LR$_{ecto}$ quaternary complex via the ensemble optimization method (EOM) (Bernadó et al., 2007) failed, most likely because of the unusually large number of degrees of freedom arising from

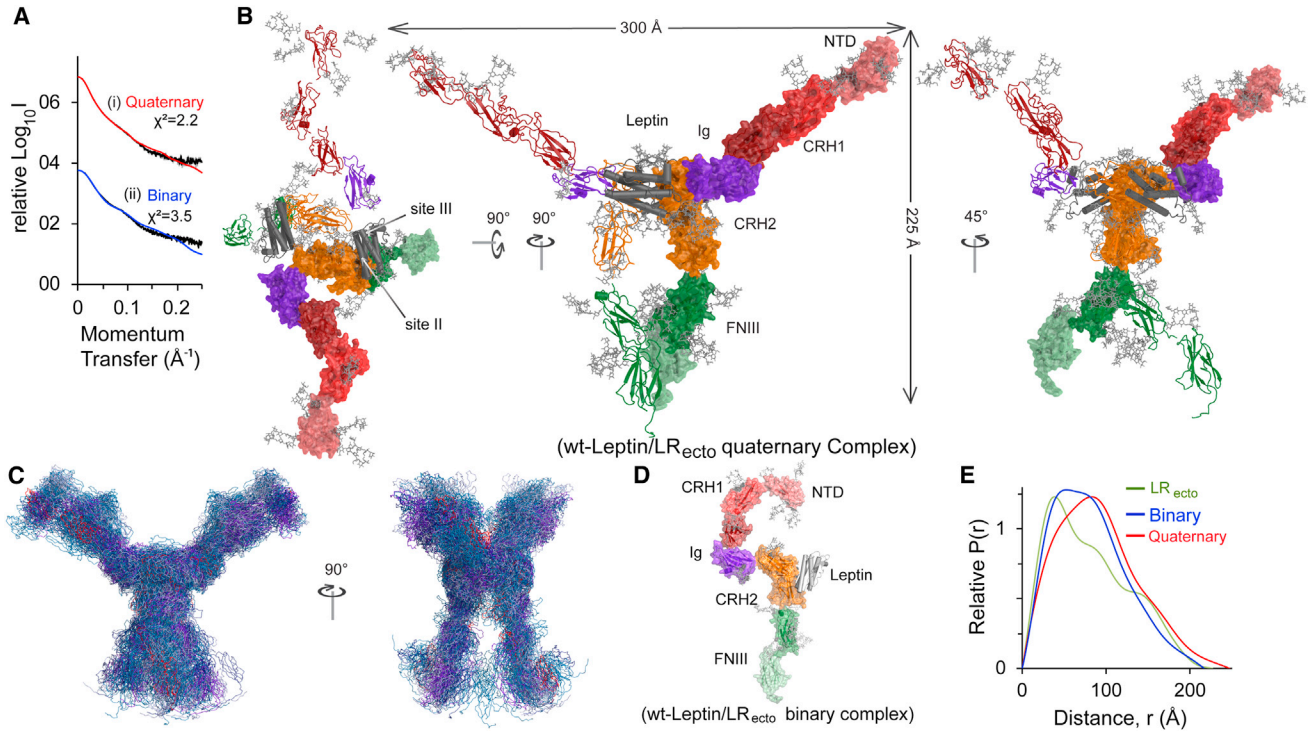

Figure 3. Structural Characterization of wt-Leptin/LR_{ecto} Complexes by SAXS

(A) Scattering curves calculated from rigid-body models of wt-leptin/LR_{ecto} quaternary complex (red) and binary complex (blue) fitted against experimental SAXS curves of quaternary (i) and binary complex (ii), respectively.

(B) Rigid-body model of the wt-leptin/LR_{ecto} quaternary complex derived from SAXS data. Leptin is shown as gray cylinders and LR_{ecto} in cartoon and surface views.

(C) LR_{ecto} domain flexibility in the wt-leptin/LR_{ecto} quaternary complex revealed from a superposition of the 50 best models of the complex (χ^2 = 2.2–2.7) derived via restrained rigid-body modeling of SAXS data. The best model is colored in pink and all other models in a gradient of blue, with darker blue representing better fitting models.

(D) Rigid-body model for the wt-leptin/LR_{ecto} binary complex derived from SAXS data.

(E) Pairwise distance-distribution plot of relative probability versus distance for LR_{ecto} (green) and wt-leptin/LR_{ecto} binary (blue) and quaternary (red) complexes. See also Figures S3 and S5.

the combination of more than 20 rigid bodies, we resorted to an alternative approach instead. Parallel modeling runs via restrained rigid-body refinement protocols implemented in SASREF and superimposition of the best 50 models confirmed an overall high degree of consistency in the models obtained and allowed us to assess the global structural flexibility and modularity of the complex (Figure 3C). Although the refined conformations for $LR_{CRH2\text{-}Ig}$ and leptin agree well in the collection of models, suggesting only moderate flexibility in the core of the complex, the relatively poor alignment in the extremities of the complex defined by LR_{CRH1} and LR_{FNIII} suggested a much greater degree of flexibility in these regions. Nonetheless, the conformational clustering of this group of models within a narrow range of χ^2 values would be consistent with an ensemble of conformers (Figure 3C). Upon extrapolating our structural studies to characterize the leptin-LR_{ecto} complex obeying 1:1 stoichiometry (Figure 3A, curve (ii), and Figure 3D) we found that this binary complex adopts a conformation that is quite different from its structure in the quaternary complex and that of unbound LR_{ecto}, as further supported by comparisons of the pair-distance distribution functions (Figure 3E).

Antagonist Leptin Variants Abrogate Ligand-Induced LR Oligomerization

Given the capacity of leptin to engage LR_{ecto} into 2:2 stoichiometric complexes, we pursued biochemical and structural insights into the possible mode of antagonism by two established antagonist leptin variants (Niv-Spector et al., 2005; Peelman et al., 2004). A parallel reasoning was that by studying LR antagonism, we might be able to obtain additional mechanistic insights into the assembly of cognate ligand-receptor complexes. One of the antagonists employed ($leptin_{a1}$) carries a S120A/T121A double mutation localizing at the beginning of helix D (Peelman et al., 2004) and was designed to interrogate the relevance of site III on leptin, while the second ($leptin_{a2}$) bears a substitution 39AAAA42 in the loop linking helices A and B and was proposed to influence the leptin-LR_{Ig} interaction (Niv-Spector et al., 2005). We note that the two sets of mutations cluster close to each other on the leptin scaffold, as the AB loop traverses the start of helix D.

Analyses by SEC-MALS of $leptin_{a1}$-LR_{ecto} and $leptin_{a2}$-LR_{ecto} complexes revealed that in contrast to wt-leptin, the two antagonist leptin variants are only able to engage LR_{ecto} in a complex obeying 1:1 stoichiometry (Figure 4A). Interestingly,

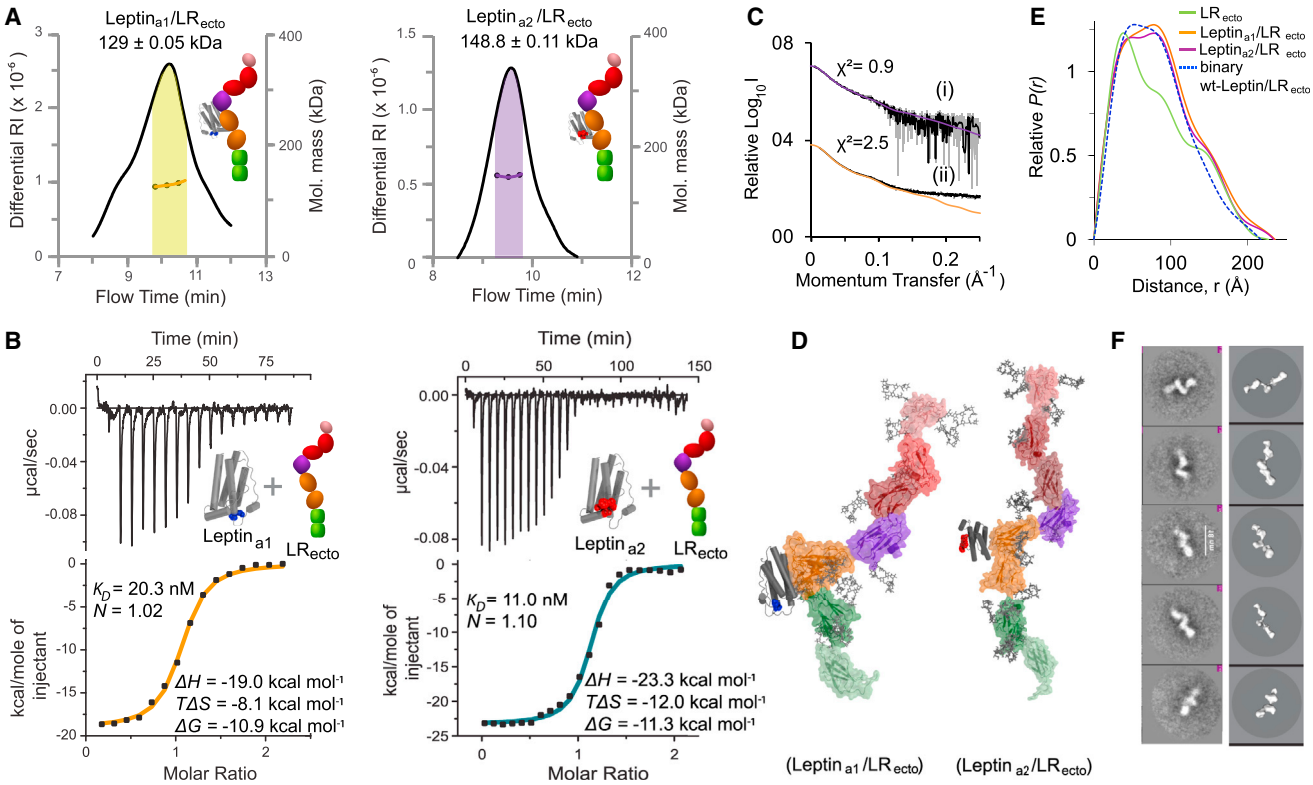

Figure 4. Biophysical and Structural Characterization of Leptin$_{a1}$/LR$_{ecto}$ and Leptin$_{a2}$/LR$_{ecto}$ Complexes

(A) SEC-MALS of leptin$_{a1}$/LR$_{ecto}$ and leptin$_{a2}$/LR$_{ecto}$ complexes.

(B) ITC thermograms of leptin$_{a1}$ and leptin$_{a2}$ binding to LR$_{ecto}$.

(C) Plot of theoretical scattering intensity from rigid-body models of leptin$_{a1}$/LR$_{ecto}$ (orange) and leptin$_{a2}$/LR$_{ecto}$ (violet) fitted to the experimental scattering (black) from the respective complexes.

(D) Rigid-body models of leptin$_{a1}$/LR$_{ecto}$ and leptin$_{a2}$/LR$_{ecto}$ binary complexes. The color scheme is as in Figure 3.

(E) Pairwise distance distribution plot of relative probability versus distance for LR$_{ecto}$ (green), leptin$_{a1}$/LR$_{ecto}$ (orange), leptin$_{a2}$/LR$_{ecto}$ (red), and binary complex of wt-leptin/LR$_{ecto}$ (dotted blue).

(F) Class averages of leptin$_{a2}$/LR$_{ecto}$ as revealed by negative-stain EM (left). Shown are five class averages of a total of seven (about 50 particles averaged per class) selected from a total of 391 particles. Also shown to the right of each class average is the ab initio model from SAXS in comparable orientation.

See also Figures S4 and S5.

the thermodynamic binding fingerprints for both antagonists (Figure 4B) are very similar to that for wt-leptin (Figure 2B), suggesting that the driving force for the assembly of the wt-leptin complex with LR$_{ecto}$ is the interaction with LR$_{CRH2}$ via site II. Structural modeling of the two binary complexes via ab initio and rigid-body modeling of SAXS data (Figures 4C–4E; Figure S4; Table 2) and leptin$_{a2}$-LR via negative-stain EM (Figure 4F) led to molecular complexes that strongly resemble the binary complex of wt-leptin with LR$_{ecto}$ in 1:1 stoichiometry (Figure 3D), as further evidenced by comparisons of the pairwise distance distribution function (Figure 4E). Thus, we can now confirm that leptin$_{a1}$ does target site III of leptin and that leptin$_{a2}$ also appears to behave as a site III antagonist, thereby pointing to the mechanistic importance of this interaction in mediating agonist-induced LR dimerization.

Free Cysteines in LR$_{ecto}$ May Constitute Conformational Switches for Activation

Delineation of the disulfide-bond network in human LR$_{ecto}$ has shown that LR$_{ecto}$ carries ten free cysteines (Haniu et al., 1998). Six of these are conserved in mouse LR$_{ecto}$, and at least one of them, Cys672, found in the membrane proximal FNIII domain, was shown to be essential for receptor activation (Zabeau et al., 2005). Interestingly, the recent crystal structure of LR$_{CRH2}$ in complex with a Fab fragment (Carpenter et al., 2012) provided insights leading to the proposal that a Cys604-Cys672 intrareceptor disulfide might be important for receptor activation. In this study, we mutated Cys604 in LR$_{CRH2}$ close to the LR$_{CRH2}$-LR$_{FNIII}$ domain boundary to serine and found that the mutant receptor can be activated only at very high leptin concentrations (>500 ng/ml), as measured by rat pancreatitis associated protein 1 (rPAP1)-luciferase reporter activity. Thus, both Cys604 and Cys672 appear to be important for receptor activation. We further note that our refined model for the 2:2 leptin-LR$_{ecto}$ complex (Figure 3) does not foster any restraints for the coupling of Cys604 and Cys672 into a disulfide at the interface of the CRH2 domains, and yet the two CRH2 domains refine to positions that allow Cys604 and Cys672 to face each other poised for such an interaction. To extend these studies and to obtain insights into the general relevance of unpaired cysteines

Table 2. SAXS Analysis of LR_{ecto} in Complex with the Leptin Antagonists $Leptin_{a1}$ and $Leptin_{a2}$

Parameter	$Leptin_{a1}/LR_{ecto}$ (Binary Complex)	$Leptin_{a2}/LR_{ecto}$ (Binary Complex)
Data Collection Parameters		
Beamline	ID 14-3, ESRF	ID 14-3, ESRF
Detector	PILATUS 1M	PILATUS 1M
Beam geometry (mm^2)	0.7 × 0.7	0.7 × 0.7
Wavelength (Å)	0.931	0.931
q range ($Å^{-1}$)	0.15–6.11	0.15–6.11
Exposure time (s)	100 (10 × 10)	100 (10 × 10)
Concentration range (mg/ml)	0.9–2.7	0.7–7.5
Temperature (K)	293	293
Structural Parameters		
I_0 ($Å^{-1}$) (from P[r])	145.9 ± 6.2	35.7 ± 2.4
R_g (Å) (from P[r])	69.1 ± 0.7	68.6 ± 2.8
I_0 ($Å^{-1}$) (from Guinier)	146.1 ± 6.5	51.0 ± 3.6
R_g (Å) (from Guinier)	67.7 ± 0.8	67.0 ± 3.8
D_{max} (Å)	236.4 ± 0.3	234.0 ± 1.5
Porod volume estimate, V_p ($Å^3$)	286,541	273,948
Excluded volume, V_{ex} ($Å^3$)	372,000	390,000
Molecular Mass (kDa)		
From I_0	140.9 ± 6.0	155.1 ± 10.5
From SAXSMoW	164.9	151.7
Protein sequence (Protparam)	109	109
Protein sequence + N-glycans	140	140
Modeling Parameters		
Symmetry	P1	P1
χ^2 of reference model	1.3	0.8
Number of models averaged	20	20
DAMAVER NSD (var)	1.02 ± 0.06	0.82 ± 0.05
Initial χ^2	3.3	0.9
Final χ^2	2.5	0.9
Software/Server		
Data reduction	BSX-CUBE	BSX-CUBE
Data processing	PRIMUS	PRIMUS
Data evaluation	PRIMUS, GNOM	PRIMUS, GNOM
Structure modeling (ab initio)	DAMMIF	DAMMIF
Structure modeling (rigid body)	SASREF	SASREF

in the conformational competence of LR_{ecto} toward complex formation, we alkylated the free cysteines in LR_{ecto} using iodoacetamide. We discovered that although the acetylated receptor could readily form a 1:1 complex with leptin, it lost its ability to undergo leptin-dependent dimerization to form a 2:2 quaternary complex (Table S1 and Figure S5). These alkylated binary complexes bear striking resemblance to the binary complexes of leptin and antagonist leptin variants (Figures 3D and 4D). Together, these lines of evidence show that Cys604 and Cys672 are likely candidates in engaging into an intrareceptor disulfide in the context of a leptin-LR quaternary complex and receptor activation. Indeed, recent evidence for functionally relevant redox regulation of the common γ_c receptor was reported in the context of interleukin-2 mediated signaling (Metcalfe et al., 2012). We expect that these insights will inspire future studies to delineate the role of unpaired cysteines in LR_{ecto} in receptor activation.

DISCUSSION

The principles underlying the assembly of the leptin-mediated extracellular signaling complex of LR have remained unclear despite great advances in understanding the physiology and biomedical relevance of signaling along the leptin-LR axis (Andò and Catalano, 2012; Guo et al., 2012). Receptor oligomerization culminating with receptor activation is a well-established paradigm for many type I cytokine receptors, but the role of the activating ligand varies among receptors. Although growth hormone receptor (Gent et al., 2002) and erythropoietin receptor (Livnah et al., 1999) exist as inactive dimers at the cell surface that are activated upon ligand binding, others, such as IL-6Rα/gp130 (Boulanger et al., 2003), leukemia inhibitory factor receptor (Huyton et al., 2007), and granulocyte macrophage colony-stimulating factor receptor (Hansen et al., 2008) proceed via ligand-induced receptor oligomerization coupled to concomitant conformational changes. LR has been reported to exist as a dimer or oligomer at the cell surface (Bacart et al., 2010; Biener et al., 2005; Devos et al., 1997; White and Tartaglia, 1999), but the conformational impact of leptin binding in the assembly of signaling complexes has remained unclear.

In this study, we used diverse methods and molecular tools, including two established leptin antagonists, to provide structural and mechanistic insights into this process that now add to recent developments in the field (Carpenter et al., 2012; Mancour et al., 2012). By carrying out comparative studies of wild-type and antagonist leptins, we have shown that high-affinity binding of leptin to the CRH2 domain of LR_{ecto} leads to structural rearrangements in LR_{ecto} to prime assembly of a complex obeying 2:2 stoichiometry. This is mediated by an interaction interface between leptin participating in a given leptin:LR_{ecto} binary complex with the Ig domain of LR_{ecto} in a second 1:1 complex. Contrary to other modular cytokine-receptor complexes of similar size and complexity (Lupardus et al., 2011; Skiniotis et al., 2005; Verstraete and Savvides, 2012), the leptin-LR_{ecto} quaternary complex lacks homotypic receptor interactions. Although our binding studies revealed that both 1:1 and 2:2 complexes assemble via similar thermodynamic binding profiles and affinities, we expect that the likely decrease in the number of degrees of freedom due to the dimensionality of the cell membrane may greatly affect the thermodynamics and kinetics of the invoked interaction between site III on leptin and LR_{Ig} in a cellular context (Wu et al., 2011). In this regard, we have now provided direct evidence for the importance of this interaction by elucidating the structural basis of leptin antagonism by two leptin mutants that stall the leptin-LR interaction to 1:1 stoichiometric complexes. Indeed, the inability of $leptin_{a2}$ to elicit fluorescence resonance energy transfer (FRET) signal elevation when added to cells expressing LR with intracellular fluorescence tags (Niv-Spector et al., 2005) is consistent with the concomitant loss of oligomerization capacity when the functionality of site III is abolished. Furthermore, we have shown that LR_{ecto} lacks inherent dimerization propensity, which now uncouples the role of LR_{ecto}

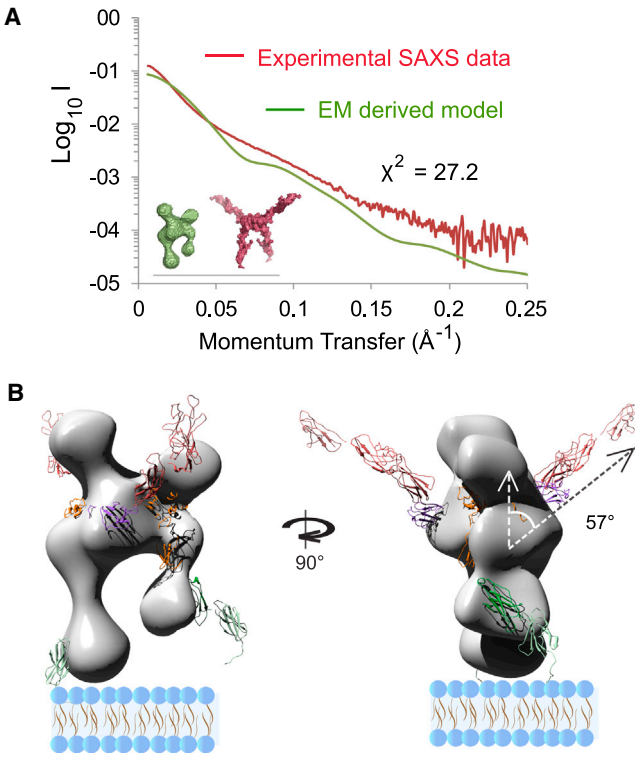

Figure 5. Comparison of SAXS-Derived and EM-Derived Models for the Leptin-LR_{ecto} Quaternary Complex

(A) Comparison of calculated scattering from a bead model derived from the previously reported EM envelope for the leptin-LR_{ecto} quaternary complex (Mancour et al., 2012) (green) and the present experimental SAXS data for the leptin-LR_{ecto} quaternary complex (raspberry). Inset: Bead model generated from the EM envelope of wt-leptin/LR_{ecto} quaternary complex (green) and major cluster center of the ab initio models from the SAXS of wt-leptin/LR_{ecto} quaternary complex (raspberry).

(B) Comparison of the SAXS-derived model for the wt-leptin/LR_{ecto} quaternary complex with the envelope for the complex derived by EM (Mancour et al., 2012).

from the assembly of constitutive, yet inactive, dimeric or oligomeric forms of LR at the cell surface in the absence of ligand (Bacart et al., 2010; Biener et al., 2005; Devos et al., 1997; White and Tartaglia, 1999).

The main question arising is whether the observed leptin-LR_{ecto} complex represents a signaling-competent assembly. An analogous complex derived by EM also obeys a 2:2 stoichiometry and has been proposed as a leptin-LR signaling complex (Mancour et al., 2012). The latter is conformationally distinct from the assembly we presented here (Figure 5). Despite the structural differences between the two assemblies, which as such can be attributed to inherent methodological limitations calling for validation via orthogonal methods, it would still be tempting to propose the observed quaternary complexes as signaling-competent states. However, we maintain that careful consideration of previous work in light of our structural data suggests otherwise.

Several studies have established that LR exists predominantly as a constitutive dimer at the cell surface (Bacart et al., 2010; Bahrenberg et al., 2002; Biener et al., 2005; Couturier and Jockers, 2003; Devos et al., 1997; White and Tartaglia, 1999).

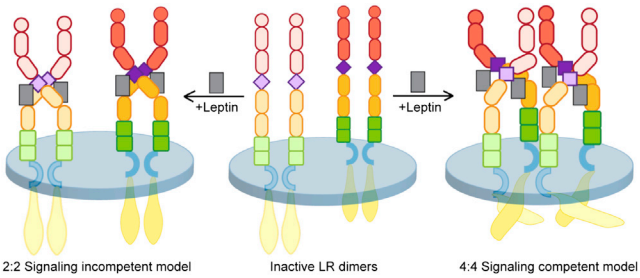

Figure 6. Proposed Mechanism for LR Activation

LR is preassembled as inactive dimer on the cell membrane (center). Leptin-induced activation can proceed through a *cis*-activation or a transactivation model. In the *cis*-activation model (left), leptin interacts with the predimerized receptor to form a 2:2 complex. This process does not require de novo oligomerization; only ligand-induced conformational changes within the receptor dimer lead to the signaling complex. Such a signaling complex model (Mancour et al., 2012) is not consistent with previous findings on the requirement for more than two LR molecules for the formation of the signaling complex (Zabeau et al., 2004). The transactivation model (right) results from ligand-induced transdimerization of two preformed LR dimers, forming a 4:4 signaling complex. This model is compatible with the requirement for more than two copies of LR in a signaling complex (Zabeau et al., 2004). Red circles denote NTD and red cylinders denote CRH1, purple denotes Ig, orange denotes CRH2, green denotes FNIII, and gray denotes leptin.

In addition, quantitative FRET based on acceptor photobleaching and fluorescence lifetime imaging microscopy on single cells (Biener et al., 2005) had suggested ligand-induced conformational changes and de novo oligomerization of LR in situ. Thus, considering constitutive LR dimers as basal assemblies for the nucleation of signaling complexes and leptin's ability to dimerize LR_{ecto} in vitro, we propose that the model most consistent with a higher order assembly would be a complex obeying 4:4 stoichiometry (Figure 6). According to this model, which contrasts previous proposals (Mancour et al., 2012; Peelman et al., 2006), binding of leptin to predimerized but inactive LR at the cell surface induces transdimerization of LR dimers to establish a signaling-competent complex. Importantly, such an assembly paradigm would be consistent with the observed weakly dominant negative repression of LR signaling by the short form of non-signaling LR (Devos et al., 1997; White et al., 1997) in the context of heteromeric LR dimers at the cell surface (Bacart et al., 2010) and supports previous studies using JAK-STAT signaling complementation (Zabeau et al., 2004). Finally, our proposed mechanistic paradigm further highlights the therapeutic importance of leptin antagonist variants that can abrogate such assemblies while displaying near wild-type affinities to LR. We envisage that the present mechanistic proposal for leptin-mediated activation of LR will set the stage for a more targeted mechanistic interrogation of the system as well as renewed efforts in antagonist development.

EXPERIMENTAL PROCEDURES

Expression and Purification of Recombinant Proteins

HEK293T cells were transiently transfected with pMET7 vector carrying cDNA for LR_{ecto} and were cultured in Dulbecco's modified Eagle's medium in the presence of penicillin (Sigma), streptomycin (Sigma), and the mannosidase inhibitor kifunensine (Tocris Bioscience) for 4 days at 37°C under 5% CO_2. The medium was harvested by centrifugation at 10,000 × *g* and filtered using

a 0.2 μm bottle-top filter. The secreted receptor was captured as a His-tagged protein on a TALON resin (Clontech), washed with 4 mM imidazole (Sigma Aldrich), and eluted with 300 mM imidazole. Purified LR_{ecto} was pooled and concentrated to 1 ml and was further purified on a Superdex 200 HiLoad 16/600 column (GE Healthcare) pre-equilibrated with buffer containing 25 mM HEPES (pH 7.4) and 100 mM sodium chloride.

Expression constructs for wt-leptin, antagonist $leptin_{a1}$ (carrying a S120A/T121A double mutation), antagonist $leptin_{a2}$ (bearing a substitution 39AAAA42) were established in the pET-11a vector, and the recombinant proteins were produced in *E. coli* as inclusion bodies. Washed inclusion bodies were solubilized in 7 M urea, and recombinant proteins were refolded in vitro by dialysis to remove urea. This preparation was further purified by ion-exchange chromatography on an ANX FF column (GE Healthcare) and by SEC using a HiLoad Superdex75 column (GE Healthcare).

Purified LR_{ecto} and wild-type or antagonist leptins were concentrated to 8 and 5 mg/ml, respectively. LR_{ecto} was mixed with a 6-fold molar excess of ligand, and the mixture was incubated at room temperature for 1 hr, followed by injection onto a pre-equilibrated Superdex 200 HiLoad 16/600 column. In the case of wt-leptin, the resulting binary and quaternary complex peaks were pooled separately for further studies.

To prepare alkylated LR_{ecto} via its free cysteine sulfhydryls, purified LR_{ecto} was incubated with 5 mM iodoacetamide for 1 hr. Complex formation with leptin and antagonist leptins was carried out as for unmodified LR_{ecto}.

Immunoprecipitation and Western Blot of Full-Length LR at the Cell Surface

HEK293T cells were seeded and after 1 day were transfected with pMET7 vector encoding murine LR with a C-terminal FLAG tag. After 24 hr, cells were washed with PBS and cultured further with 10% fetal calf serum (Sigma Aldrich). For cell-surface biotinylation, cells were detached with trypsin and washed three times with ice-cold PBS. Cells were resuspended to 25×10^6 cells/ml and treated with 0.1% azide to prevent internalization of cell-surface receptors. Cells were incubated at room temperature with freshly prepared 0.8 mM sulfo-NHS-SS for 30 min. To remove unreacted biotin, cells were washed with ice-cold PBS containing 0.1% azide. Cells were lysed using modified radioimmunoprecipitation assay buffer containing 50 mM iodoacetamide, to prevent nonphysiological clustering during processing, and lysate was cleared by centrifuging for 10 min at 14,000 rpm. To enrich biotinylated LR using Dymabeads Streptavidin T1 (Invitrogen), beads were washed three times with PBS, cleared lysate was added to the beads, and the mixture was incubated at room temperature for 30 min while rotating and washed three times with PBS containing 0.1% (v/v) Tween-20 (Sigma). Biotinylated LR was eluted with Laemmli buffer. For detection, samples were heated at 65°C for 5 min and resolved on 7.5% SDS-PAGE with and without 2-mercaptoethanol. LR was detected via western blot using an anti-FLAG antibody (Sigma).

Chemical Crosslinking of LR_{ecto}/wt-Leptin Complex

Thirty microliters of 36.5% to 38% aqueous solution of formaldehyde (Sigma) was diluted in 1 M HEPES (pH 7.4) to a final volume of 100 μl. Then 5 μl of this diluted formaldehyde was added to 40 μl of wt-leptin/LR_{ecto} quaternary complex at 0.3 to 0.8 μM and adjusted to a final volume of 50 μl with buffer containing 50 mM HEPES (pH 7.4) and 100 mM sodium chloride, followed by a 3 hr incubation at room temperature. The crosslinking reaction was stopped by adding 1 M Tris (pH 7.4). This sample was further analyzed on nonreducing SDS-PAGE, followed by silver staining to assess the efficiency of crosslinking.

ITC

All protein components were purified in 25 mM HEPES (pH 7.4) containing 100 mM sodium chloride and degassed immediately before titration. Then 20 μM of wt-leptin was titrated against 1.4 ml of 1 μM LR_{ecto} with 17 discrete injections (3 μl followed by 10 μl each) at 37°C and mixing at 307 rpm stirring speed. The heat released was recorded using a MicroCal VP-ITC setup (GE Healthcare) and analyzed using Origin (OriginLab). The best fitting of the experimental data were obtained using a "one set of sites" curve fitting model in Origin, and this fit was used to determine the equilibrium dissociation constant (K_D), the stoichiometry of the interaction (N), and the enthalpy change (ΔH). The change in Gibbs free energy (ΔG) was calculated using the equation $\Delta G = -RT \ln(1/K_D)$, and the entropy change (ΔS) was calculated as $\Delta G = \Delta H - T\Delta S$.

Similar experiments were performed for $leptin_{a1}$ and $leptin_{a2}$ to characterize their interactions with LR_{ecto}. In order to verify the stoichiometry of the high molecular weight complex, a similar protocol was followed using a MicroCal ITC_{200} instrument by titrating wt-leptin at 2.4 mg/ml (~148 μM) into LR_{ecto} at 1.2 mg/ml (~8.4 μM).

Binding and Signaling Properties of LR_{C604S}

Cys604 in mouse LR was mutated into a serine using standard site-directed mutagenesis techniques and was cloned into the pMET7 expression vector. pMET7-LR_{C604S} was transfected together with the pXP2d2-rPAP1-luciferase reporter (Eyckerman et al., 2000) into HEK293T cells with calcium phosphate. Cells were stimulated overnight with a serial dilution of leptin and lysed, and light emission was measured in a TopCount chemiluminescence counter (PerkinElmer). Leptin binding was determined using the leptin-secreted alkaline phosphatase chimera, as described earlier (Zabeau et al., 2005). In brief, transfected cells are incubated with fusion-protein for 2 hr. After three washing steps, bound enzymatic activity is measured with the Phospha-Light assay (Life Technologies) in the TopCount counter.

MALS

The molecular masses, oligomerization state of LR_{ecto}, and its complexes with wt-leptin, $leptin_{a1}$, and $leptin_{a2}$ in a concentration range of 18 to 50 μM were estimated using MALS. Purified protein samples were resolved on an asymmetric FFF system (Wyatt Technology) encompassing an ultrafiltration membrane (Microdyn-Nadir) with a 10 kDa cutoff and a spacer with a height of 350 μm, a high-performance liquid chromatography (HPLC) unit (Shimadzu), an online UV detector (Shimadzu), a static light scattering detector (DAWN HELEOS), and a refractometer (Optilab T-rEX; Wyatt Technology). To enhance peak resolution for the wt-leptin/LR_{ecto} complex during FFF elution, the cross-flow was optimized. On the basis of the measured Rayleigh scattering at different angles and the established differential refractive index increment of 0.185 mL/g for proteins in solution with respect to the change in protein concentration (dn/dc) (Graupner et al., 1999), weight-averaged molar masses for each species were calculated using ASTRA V software.

SAXS

Data Collection and Processing

SAXS data were measured at beamline SWING at SOLEIL Synchrotron (Gif-sur-Yvette, France) with a mounted online HPLC system (David and Perez, 2009) and beamline ID14-3 of the European Synchrotron Radiation Facility (ESRF; Grenoble, France). Purified LR_{ecto} and its binary complexes with $leptin_{a1}$ and $leptin_{a2}$ were measured in bulk mode at 3 different concentrations in the range of 0.5 to 3 mg/ml. wt-Leptin/LR_{ecto} complex at 10 mg/ml was first resolved on an online gel-filtration column (Shodex KW404-4F). X-ray scattering data were recorded within a momentum transfer range of $0.01\ Å^{-1} < s < 0.6\ Å^{-1}$, where $s = 4\pi\sin\theta/\lambda$. X-ray-induced radiation damage was evaluated by superposition of ten scattering curves obtained from integration of continuous radial scattering obtained from independent measurements with 10 s exposure for each sample. For each concentration set, the scattering data were normalized for beam intensity and exposure time and corrected for the detector response. Subtraction of buffer scattering from the sample scattering using PRIMUS (Konarev et al., 2003) eliminated both buffer background and background arising from instrument hardware. After resolution of wt-leptin/LR_{ecto} on a size-exclusion column, 150 frames with exposure time of 1 s and delay of 0.5 s each were collected for buffer, followed by measurements for the protein peak. The forward scattering (I_0) and radius of gyration (R_g) were determined in PRIMUS from infinite dilution extrapolation on the basis of Guinier approximation and compared with corresponding estimates from Gnom (Svergun, 1992). The distance distribution function P(r) and maximal dimension D_{max} for each scatterer were evaluated using Gnom. Molecular masses were calculated on the basis of the forward scattering from a calibrated sample employing BSA (ID14-3, ESRF) or water (Swing, SOLEIL) and independent of calibration standards using SAXSMoW (Fischer et al., 2010). Porod volumes were estimated using Autoporod (Petoukhov et al., 2012).

Ab Initio Modeling

Three-dimensional shape reconstructions were generated via DAMMIF (Franke and Svergun, 2009), and 20 models were generated via independent

runs for each scatterer type. Model uniqueness was evaluated using DAMAVER (Volkov and Svergun, 2003). When the average normalized spatial discrepancy (NSD) value for the 20 models was $\leq$1, the set was considered a single cluster, and the model with the lowest NSD average value with respect to the other 19 models was considered representative of the scatterer type. However, for the wt-leptin/LR_{ecto} complex, average NSD values were ~1.6. Visual inspection of these models confirmed variability in the models, possibly because of the flexibility of this system. The models were clustered using DAMCLUST, and the cluster centers were considered the representative conformers of the wt-leptin/LR_{ecto} quaternary complex.

Rigid-Body Modeling

Restrained rigid-body refinement of models against the SAXS data was carried out via SASREF (Petoukhov and Svergun, 2005). The 3D models for eight individual receptor structural domains (three for CRH1, one for Ig, two for CRH2, and two for FNIII) were generated as described previously (Peelman et al., 2006), except for CRH1 and FNIII, which were predicted using I-TASSER (Roy et al., 2010, 2012). On the basis of the earlier experimental evidence for the sites of glycosylation on LR_{ecto} (Haniu et al., 1998) and further predicted N-glycosylation sites on individual domain predicted structures, these were glycosylated in silico using GlyProt server (Bohne-Lang and von der Lieth, 2005). The best results were obtained when two $GlcNAc_2Man_9$ trees (glycan id: 9146) were used for in silico glycosylation. The distance between Cα atoms of the C and N termini in consecutive domains was restricted to 3.7 Å. Initial ligand-receptor and receptor-receptor domain distances were based on the proposed model for the leptin-LR complex (Peelman et al., 2006) and were optimized in subsequent rounds of modeling. The quaternary leptin/LR_{ecto} complex with 2:2 stoichiometry was modeled with P2 symmetry restraints, while modeling of all other SAXS data for LR_{ecto}, $leptin_{a1}$-LR_{ecto}, and $leptin_{a2}$-LR_{ecto} complex was carried out under P1 symmetry. Model quality was assessed using Crysol (Svergun et al., 1995).

Negative-Stain EM

Samples were diluted in base buffer (25 mM HEPES [pH 7.4] containing 100 mM sodium chloride) as required and adsorbed for 1 min to glow discharged thin carbon films coating a perforated carbon layer on gold-coated copper grids. These were washed with four drops of distillated water and negatively stained with 2% (w/v) uranyl acetate and imaged with a CM10 transmission electron microscope (Philips) operating at 80 kV. Electron micrographs were recorded with a 2k charge-coupled device camera (Veleta; Olympus Soft Imaging Solutions) at a nominal magnification of 130,000×, yielding a final pixel size corresponding to 0.37 nm on the specimen scale. Particles were manually selected for single-particle analysis and averaged using EMAN software (Ludtke et al., 1999).

SUPPLEMENTAL INFORMATION

Supplemental Information includes five figures and one table and can be found with this article online at http://dx.doi.org/10.1016/j.str.2014.04.012.

ACKNOWLEDGMENTS

This work was supported by a Methusalem grant (Ghent University, Ghent, Belgium) and by Fonds Wetenschappelijk Onderzoek (Brussels, Belgium). J.T. is holder of an ERC Advanced Grant (340941). We are grateful to the ESRF, SOLEIL, and Deutsches Elektronen-Synchrotron/European Molecular Biology Laboratory for access to synchrotron facilities and data collection support. We thank the SWITCH laboratory (Vlaams Instituut voor Biotechnologie [VIB], Ghent, Belgium) and Dr. Rodrigo Gallardo (VIB) for access to and assistance with MALS measurements. Prof. Georgios Skiniotis (University of Michigan) kindly provided the EM map derived for the leptin-LR quaternary complex for comparison purposes.

Received: November 7, 2013
Revised: April 17, 2014
Accepted: April 24, 2014
Published: May 29, 2014

REFERENCES

Andò, S., and Catalano, S. (2012). The multifactorial role of leptin in driving the breast cancer microenvironment. Nat. Rev. Endocrinol. *8*, 263–275.

Artac, M., and Altundag, K. (2012). Leptin and breast cancer: an overview. Med. Oncol. *29*, 1510–1514.

Bacart, J., Leloire, A., Levoye, A., Froguel, P., Jockers, R., and Couturier, C. (2010). Evidence for leptin receptor isoforms heteromerization at the cell surface. FEBS Lett. *584*, 2213–2217.

Bahrenberg, G., Behrmann, I., Barthel, A., Hekerman, P., Heinrich, P.C., Joost, H.G., and Becker, W. (2002). Identification of the critical sequence elements in the cytoplasmic domain of leptin receptor isoforms required for Janus kinase/signal transducer and activator of transcription activation by receptor heterodimers. Mol. Endocrinol. *16*, 859–872.

Bernadó, P., Mylonas, E., Petoukhov, M.V., Blackledge, M., and Svergun, D.I. (2007). Structural characterization of flexible proteins using small-angle X-ray scattering. J. Am. Chem. Soc. *129*, 5656–5664.

Biener, E., Charlier, M., Ramanujan, V.K., Daniel, N., Eisenberg, A., Bjorbaek, C., Herman, B., Gertler, A., and Djiane, J. (2005). Quantitative FRET imaging of leptin receptor oligomerization kinetics in single cells. Biol. Cell. *97*, 905–919.

Bohne-Lang, A., and von der Lieth, C.W. (2005). GlyProt: in silico glycosylation of proteins. Nucleic Acids Res. *33* (Web Server issue), W214–W219.

Boulanger, M.J., Chow, D.C., Brevnova, E.E., and Garcia, K.C. (2003). Hexameric structure and assembly of the interleukin-6/IL-6 alpha-receptor/gp130 complex. Science *300*, 2101–2104.

Cao, R., Brakenhielm, E., Wahlestedt, C., Thyberg, J., and Cao, Y. (2001). Leptin induces vascular permeability and synergistically stimulates angiogenesis with FGF-2 and VEGF. Proc. Natl. Acad. Sci. USA *98*, 6390–6395.

Carbone, F., La Rocca, C., and Matarese, G. (2012). Immunological functions of leptin and adiponectin. Biochimie *94*, 2082–2088.

Carpenter, B., Hemsworth, G.R., Wu, Z., Maamra, M., Strasburger, C.J., Ross, R.J., and Artymiuk, P.J. (2012). Structure of the human obesity receptor leptin-binding domain reveals the mechanism of leptin antagonism by a monoclonal antibody. Structure *20*, 487–497.

Chang, V.T., Crispin, M., Aricescu, A.R., Harvey, D.J., Nettleship, J.E., Fennelly, J.A., Yu, C., Boles, K.S., Evans, E.J., Stuart, D.I., et al. (2007). Glycoprotein structural genomics: solving the glycosylation problem. Structure *15*, 267–273.

Couturier, C., and Jockers, R. (2003). Activation of the leptin receptor by a ligand-induced conformational change of constitutive receptor dimers. J. Biol. Chem. *278*, 26604–26611.

Cummings, B.P., Bettaieb, A., Graham, J.L., Stanhope, K.L., Dill, R., Morton, G.J., Haj, F.G., and Havel, P.J. (2011). Subcutaneous administration of leptin normalizes fasting plasma glucose in obese type 2 diabetic UCD-T2DM rats. Proc. Natl. Acad. Sci. USA *108*, 14670–14675.

David, G., and Perez, J. (2009). Combined sampler robot and high-performance liquid chromatography: a fully automated system for biological small-angle X-ray scattering experiments at the Synchrotron SOLEIL SWING beamline. J. Appl. Cryst. *42*, 892–900.

De Rosa, V., Procaccini, C., Calì, G., Pirozzi, G., Fontana, S., Zappacosta, S., La Cava, A., and Matarese, G. (2007). A key role of leptin in the control of regulatory T cell proliferation. Immunity *26*, 241–255.

Devos, R., Guisez, Y., Van der Heyden, J., White, D.W., Kalai, M., Fountoulakis, M., and Plaetinck, G. (1997). Ligand-independent dimerization of the extracellular domain of the leptin receptor and determination of the stoichiometry of leptin binding. J. Biol. Chem. *272*, 18304–18310.

Elegheert, J., Bracke, N., Pouliot, P., Gutsche, I., Shkumatov, A.V., Tarbouriech, N., Verstraete, K., Bekaert, A., Burmeister, W.P., Svergun, D.I., et al. (2012). Allosteric competitive inactivation of hematopoietic CSF-1 signaling by the viral decoy receptor BARF1. Nat. Struct. Mol. Biol. *19*, 938–947.

Eyckerman, S., Broekaert, D., Verhee, A., Vandekerckhove, J., and Tavernier, J. (2000). Identification of the Y985 and Y1077 motifs as SOCS3 recruitment sites in the murine leptin receptor. FEBS Lett. *486*, 33–37.

Felix, J., Elegheert, J., Gutsche, I., Shkumatov, A.V., Wen, Y., Bracke, N., Pannecoucke, E., Vandenberghe, I., Devreese, B., Svergun, D.I., et al. (2013). Human IL-34 and CSF-1 establish structurally similar extracellular assemblies with their common hematopoietic receptor. Structure *21*, 528–539.

Fischer, H., de Oliveira Neto, M., Napolitano, H.B., Polikarpov, I., and Craievich, A.F. (2010). Determination of the molecular weight of proteins in solution from a single small-angle X-ray scattering measurement on a relative scale. J. Appl. Cryst. *43*, 101–109.

Fong, T.M., Huang, R.R., Tota, M.R., Mao, C., Smith, T., Varnerin, J., Karpitskiy, V.V., Krause, J.E., and Van der Ploeg, L.H. (1998). Localization of leptin binding domain in the leptin receptor. Mol. Pharmacol. *53*, 234–240.

Franke, D., and Svergun, D.I. (2009). DAMMIF, a program for rapidab-initioshape determination in small-angle scattering. J. Appl. Cryst. *42*, 342–346.

Friedman, J.M., and Halaas, J.L. (1998). Leptin and the regulation of body weight in mammals. Nature *395*, 763–770.

Gent, J., van Kerkhof, P., Roza, M., Bu, G., and Strous, G.J. (2002). Ligand-independent growth hormone receptor dimerization occurs in the endoplasmic reticulum and is required for ubiquitin system-dependent endocytosis. Proc. Natl. Acad. Sci. USA *99*, 9858–9863.

Gertler, A. (2006). Development of leptin antagonists and their potential use in experimental biology and medicine. Trends Endocrinol. Metab. *17*, 372–378.

Ghilardi, N., and Skoda, R.C. (1997). The leptin receptor activates janus kinase 2 and signals for proliferation in a factor-dependent cell line. Mol. Endocrinol. *11*, 393–399.

Graupner, M., Haalck, L., Spener, F., Lindner, H., Glatter, O., Paltauf, F., and Hermetter, A. (1999). Molecular dynamics of microbial lipases as determined from their intrinsic tryptophan fluorescence. Biophys. J. *77*, 493–504.

Guo, S., Liu, M., Wang, G., Torroella-Kouri, M., and Gonzalez-Perez, R.R. (2012). Oncogenic role and therapeutic target of leptin signaling in breast cancer and cancer stem cells. Biochim. Biophys. Acta *1825*, 207–222.

Guttman, M., Weinkam, P., Sali, A., and Lee, K.K. (2013). All-atom ensemble modeling to analyze small-angle x-ray scattering of glycosylated proteins. Structure *21*, 321–331.

Halaas, J.L., Gajiwala, K.S., Maffei, M., Cohen, S.L., Chait, B.T., Rabinowitz, D., Lallone, R.L., Burley, S.K., and Friedman, J.M. (1995). Weight-reducing effects of the plasma protein encoded by the obese gene. Science *269*, 543–546.

Haniu, M., Arakawa, T., Bures, E.J., Young, Y., Hui, J.O., Rohde, M.F., Welcher, A.A., and Horan, T. (1998). Human leptin receptor. Determination of disulfide structure and N-glycosylation sites of the extracellular domain. J. Biol. Chem. *273*, 28691–28699.

Hansen, G., Hercus, T.R., McClure, B.J., Stomski, F.C., Dottore, M., Powell, J., Ramshaw, H., Woodcock, J.M., Xu, Y., Guthridge, M., et al. (2008). The structure of the GM-CSF receptor complex reveals a distinct mode of cytokine receptor activation. Cell *134*, 496–507.

Hausman, G.J., Barb, C.R., and Lents, C.A. (2012). Leptin and reproductive function. Biochimie *94*, 2075–2081.

Huyton, T., Zhang, J.G., Luo, C.S., Lou, M.Z., Hilton, D.J., Nicola, N.A., and Garrett, T.P. (2007). An unusual cytokine:Ig-domain interaction revealed in the crystal structure of leukemia inhibitory factor (LIF) in complex with the LIF receptor. Proc. Natl. Acad. Sci. USA *104*, 12737–12742.

Iserentant, H., Peelman, F., Defeau, D., Vandekerckhove, J., Zabeau, L., and Tavernier, J. (2005). Mapping of the interface between leptin and the leptin receptor CRH2 domain. J. Cell Sci. *118*, 2519–2527.

Konarev, P.V., Volkov, V.V., Sokolova, A.V., Koch, M.H.J., and Svergun, D.I. (2003). PRIMUS: a Windows PC-based system for small-angle scattering data analysis. J. Appl. Cryst. *36*, 1277–1282.

Leitner, A., Walzthoeni, T., Kahraman, A., Herzog, F., Rinner, O., Beck, M., and Aebersold, R. (2010). Probing native protein structures by chemical cross-linking, mass spectrometry, and bioinformatics. Mol. Cell. Proteomics *9*, 1634–1649.

Livnah, O., Stura, E.A., Middleton, S.A., Johnson, D.L., Jolliffe, L.K., and Wilson, I.A. (1999). Crystallographic evidence for preformed dimers of erythropoietin receptor before ligand activation. Science *283*, 987–990.

Lu, X.Y., Kim, C.S., Frazer, A., and Zhang, W. (2006). Leptin: a potential novel antidepressant. Proc. Natl. Acad. Sci. USA *103*, 1593–1598.

Ludtke, S.J., Baldwin, P.R., and Chiu, W. (1999). EMAN: semiautomated software for high-resolution single-particle reconstructions. J. Struct. Biol. *128*, 82–97.

Lupardus, P.J., Skiniotis, G., Rice, A.J., Thomas, C., Fischer, S., Walz, T., and Garcia, K.C. (2011). Structural snapshots of full-length Jak1, a transmembrane gp130/IL-6/IL-6Rα cytokine receptor complex, and the receptor-Jak1 holocomplex. Structure *19*, 45–55.

Mancour, L.V., Daghestani, H.N., Dutta, S., Westfield, G.H., Schilling, J., Oleskie, A.N., Herbstman, J.F., Chou, S.Z., and Skiniotis, G. (2012). Ligand-induced architecture of the leptin receptor signaling complex. Mol. Cell *48*, 655–661.

Metcalfe, C., Cresswell, P., and Barclay, A.N. (2012). Interleukin-2 signalling is modulated by a labile disulfide bond in the CD132 chain of its receptor. Open Biol. *2*, 110036.

Motyl, K.J., and Rosen, C.J. (2012). Understanding leptin-dependent regulation of skeletal homeostasis. Biochimie *94*, 2089–2096.

Niv-Spector, L., Gonen-Berger, D., Gourdou, I., Biener, E., Gussakovsky, E.E., Benomar, Y., Ramanujan, K.V., Taouis, M., Herman, B., Callebaut, I., et al. (2005). Identification of the hydrophobic strand in the A-B loop of leptin as major binding site III: implications for large-scale preparation of potent recombinant human and ovine leptin antagonists. Biochem. J. *391*, 221–230.

Otvos, L., Jr., Kovalszky, I., Riolfi, M., Ferla, R., Olah, J., Sztodola, A., Nama, K., Molino, A., Piubello, Q., Wade, J.D., and Surmacz, E. (2011). Efficacy of a leptin receptor antagonist peptide in a mouse model of triple-negative breast cancer. Eur. J. Cancer *47*, 1578–1584.

Park, H.Y., Kwon, H.M., Lim, H.J., Hong, B.K., Lee, J.Y., Park, B.E., Jang, Y., Cho, S.Y., and Kim, H.S. (2001). Potential role of leptin in angiogenesis: leptin induces endothelial cell proliferation and expression of matrix metalloproteinases in vivo and in vitro. Exp. Mol. Med. *33*, 95–102.

Peelman, F., Van Beneden, K., Zabeau, L., Iserentant, H., Ulrichts, P., Defeau, D., Verhee, A., Catteeuw, D., Elewaut, D., and Tavernier, J. (2004). Mapping of the leptin binding sites and design of a leptin antagonist. J. Biol. Chem. *279*, 41038–41046.

Peelman, F., Iserentant, H., De Smet, A.S., Vandekerckhove, J., Zabeau, L., and Tavernier, J. (2006). Mapping of binding site III in the leptin receptor and modeling of a hexameric leptin.leptin receptor complex. J. Biol. Chem. *281*, 15496–15504.

Petoukhov, M.V., and Svergun, D.I. (2005). Global rigid body modeling of macromolecular complexes against small-angle scattering data. Biophys. J. *89*, 1237–1250.

Petoukhov, M.V., Franke, D., Shkumatov, A.V., Tria, G., Kikhney, A.G., Gajda, M., Gorba, C., Mertens, H.D.T., Konarev, P.V., and Svergun, D.I. (2012). New developments in theATSASprogram package for small-angle scattering data analysis. J. Appl. Cryst. *45*, 342–350.

Procaccini, C., Jirillo, E., and Matarese, G. (2012). Leptin as an immunomodulator. Mol. Aspects Med. *33*, 35–45.

Ramachandrappa, S., and Farooqi, I.S. (2011). Genetic approaches to understanding human obesity. J. Clin. Invest. *121*, 2080–2086.

Ring, A.M., Lin, J.X., Feng, D., Mitra, S., Rickert, M., Bowman, G.R., Pande, V.S., Li, P., Moraga, I., Spolski, R., et al. (2012). Mechanistic and structural insight into the functional dichotomy between IL-2 and IL-15. Nat. Immunol. *13*, 1187–1195.

Roy, A., Kucukural, A., and Zhang, Y. (2010). I-TASSER: a unified platform for automated protein structure and function prediction. Nat. Protoc. *5*, 725–738.

Roy, A., Yang, J., and Zhang, Y. (2012). COFACTOR: an accurate comparative algorithm for structure-based protein function annotation. Nucleic Acids Res. *40* (Web Server issue), W471–W477.

Sennello, J.A., Fayad, R., Morris, A.M., Eckel, R.H., Asilmaz, E., Montez, J., Friedman, J.M., Dinarello, C.A., and Fantuzzi, G. (2005). Regulation of T cell-mediated hepatic inflammation by adiponectin and leptin. Endocrinology *146*, 2157–2164.

Skiniotis, G., Boulanger, M.J., Garcia, K.C., and Walz, T. (2005). Signaling conformations of the tall cytokine receptor gp130 when in complex with IL-6 and IL-6 receptor. Nat. Struct. Mol. Biol. *12*, 545–551.

Svergun, D. (1992). Determination of the regularization parameter in indirect-transform methods using perceptual criteria. J. Appl. Cryst. *25*, 495–503.

Svergun, D., Barberato, C., and Koch, M.H.J. (1995). CRYSOL - a Program to Evaluate X-ray Solution Scattering of Biological Macromolecules from Atomic Coordinates. J. Appl. Cryst. *28*, 768–773.

Varela, L., and Horvath, T.L. (2012). Leptin and insulin pathways in POMC and AgRP neurons that modulate energy balance and glucose homeostasis. EMBO Rep. *13*, 1079–1086.

Verstraete, K., and Savvides, S.N. (2012). Extracellular assembly and activation principles of oncogenic class III receptor tyrosine kinases. Nat. Rev. Cancer *12*, 753–766.

Volkov, V.V., and Svergun, D.I. (2003). Uniqueness of ab initio shape determination in small-angle scattering. J. Appl. Cryst. *36*, 860–864.

Wang, X., Rickert, M., and Garcia, K.C. (2005). Structure of the quaternary complex of interleukin-2 with its alpha, beta, and gammac receptors. Science *310*, 1159–1163.

Wang, M.Y., Chen, L., Clark, G.O., Lee, Y., Stevens, R.D., Ilkayeva, O.R., Wenner, B.R., Bain, J.R., Charron, M.J., Newgard, C.B., and Unger, R.H. (2010). Leptin therapy in insulin-deficient type I diabetes. Proc. Natl. Acad. Sci. USA *107*, 4813–4819.

Wauman, J., De Smet, A.S., Catteeuw, D., Belsham, D., and Tavernier, J. (2008). Insulin receptor substrate 4 couples the leptin receptor to multiple signaling pathways. Mol. Endocrinol. *22*, 965–977.

White, D.W., and Tartaglia, L.A. (1999). Evidence for ligand-independent homo-oligomerization of leptin receptor (OB-R) isoforms: a proposed mechanism permitting productive long-form signaling in the presence of excess short-form expression. J. Cell. Biochem. *73*, 278–288.

White, D.W., Kuropatwinski, K.K., Devos, R., Baumann, H., and Tartaglia, L.A. (1997). Leptin receptor (OB-R) signaling. Cytoplasmic domain mutational analysis and evidence for receptor homo-oligomerization. J. Biol. Chem. *272*, 4065–4071.

Wu, Y., Vendome, J., Shapiro, L., Ben-Shaul, A., and Honig, B. (2011). Transforming binding affinities from three dimensions to two with application to cadherin clustering. Nature *475*, 510–513.

Zabeau, L., Defeau, D., Van der Heyden, J., Iserentant, H., Vandekerckhove, J., and Tavernier, J. (2004). Functional analysis of leptin receptor activation using a Janus kinase/signal transducer and activator of transcription complementation assay. Mol. Endocrinol. *18*, 150–161.

Zabeau, L., Defeau, D., Iserentant, H., Vandekerckhove, J., Peelman, F., and Tavernier, J. (2005). Leptin receptor activation depends on critical cysteine residues in its fibronectin type III subdomains. J. Biol. Chem. *280*, 22632–22640.

Zhang, F., Basinski, M.B., Beals, J.M., Briggs, S.L., Churgay, L.M., Clawson, D.K., DiMarchi, R.D., Furman, T.C., Hale, J.E., Hsiung, H.M., et al. (1997). Crystal structure of the obese protein leptin-E100. Nature *387*, 206–209.